

OPTIMAL ALLOCATION OF ENERGY STORAGE SYSTEM (ESS) AND UPQC BY PSO FOR GRID CONNECTED WIND MODEL

S SooriyaPrabha

Parisutham Institute of Technology and Science,
Thanjavur, Tamil Nadu
sethu25112009@gmail.com

C.K Babulal

Thiagarajar College of Engineering,
Madurai, Tamil Nadu
ckbabulal@gmail.com

Abstract

In the ambience of renewable energy integrated grid of electricity generation, the endeavor of energy storage strategy (ESS) has been an inevitable technique to abduct the energy by means of renewable sources and endow during the obligation of huge electrical energy. Inoculation of the wind power into an electric grid affects the power quality. The arbitrary arrangement of ESS in the grid integration has prompt pessimistic characteristic. Vanquishing this bothersome impact of ESS in this errand, one of the meta-heuristic portrayal particle swarm optimization (PSO) has been resolved since requires less computational stretch and depicts in MATPOWER. The proposed model outfits the ideal area of ESS in the system of electricity generation and idealistic aspect of ESS. In this paper introduces a complete audit on the unified power quality conditioner (UPQC) to improve the electric power quality at appropriation levels and also the execution of PSO over the test system relates with pertinence of optimal power flow (OPF) model with assorted investigations, to prognosis the envisage of PSO to forfeiture the unfortunate costs and real power shortfalls imports to transmission for conservative generation of electric power. In this proposed plot UPQC is associated at a state of regular coupling with a battery energy storage system (BESS) to alleviate the power quality issues. The battery energy storage is coordinated to maintain the real power source under fluctuating wind power. The UPQC control conspire for the grid associated wind energy generation system for power quality renovation is simulated using MATLAB/SIMULINK in power system block set.

Keywords: Particle swarm optimization, energy storage system, wind energy conversion system, UPQC.

1. Introduction

To have reasonable development and social advance, it is important to meet the energy require by using the renewable energy resources like wind, biomass, hydro, co-generation, etc. In feasible energy framework, energy conservation and

the utilization of renewable source are the key worldview. At the beginning, coal is the preeminent real asset used to generate the electrical energy nonetheless the need of electrical energy had expanded and after that the researchers investigate distinct resources accessible in the earth initiated to utilize the endowed sources such natural gas and non-conventional energy resources. The worldwide energy commitments by oil, gas, coal and non-fossil fuels each will be around 25% in 2040. Withal renewable energy sources are abrupt expanding and contribute around 14% of prime energy.

It has been consistently a threat to preserve the quality of electric power within the tolerable restraint [1-7]. The need to desegregate the renewable energy like wind energy into power system is to make it conceivable to limit the ecological impact on conventional plant [11]. In this framework of wind energy scheme (WES) and energy storage strategy (ESS) have been converged in the expected IEEE-30 bus test system, nevertheless the due to stochastically nature of wind, excess energy generated has been reserved in energy storage strategy. Ideal rating of the energy storage system with respect to the grid endurance examined in [8&9].

The integration of ESS determined the grid with improved power quality and has the ability to intensify the stability of the power system as apprise in [10]. The particle swarm optimization and its assorted form of algorithm were used for the best arrangement of ESS in the grid as all-inclusive in [12,13,14,15&16].

A new terminology to resolve the power quality index is disused in [17&18]. In [19] the power quality of wind associated grid is investigated utilizing wavelet packet transform. Point scheme strategy is used to examine the harmonics and quality of power as in [20]. The stability of wind turbines after they associated with the grid is resolved in [21]. The wind energy fore- casted by time series and neural

network as in [22] and ARMA (autoregressive moving average) and ANN (artificial neural networks) as described in [23]. In recent years, the technological advancement of high power electronics devices has prompted execution of electronic equipment suited for electric power systems, with quick reaction contrasted with the line frequency.

The focal point of this paper on a unified power quality condition (UPQC). The UPQC is one type of the Active Power Filter (APF) where shunt and series APF functionalities are incorporated together to accomplish better control more than several power quality issues at the same time. The UPQC is controlled to regulate the real and reactive power, voltage level at Point of Common Coupling (PCC). Simulations were carried out to demonstrate the adequacy of the proposed remuneration approach. Figure 1. Shows the general block diagram of UPQC. In the current literature, aligned such that promulgation of the wind probability has been detailed section 2 followed by objective function of the projected algorithm has been discussed in section 3. The meta-heuristic model of particle swarm optimization and its application has been illustrated in section 4. At last the final section oriented towards the elucidation about the deduction of the investigation.

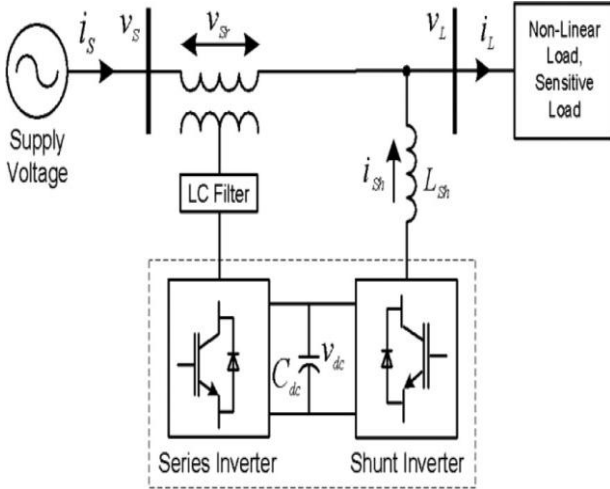


Fig. 1. UPQC general block diagram representation

2. Probabilistic in dissemination of wind

The power from WECS is stochastic in nature attributable to changing pace of the wind in the land territory. In this analysis, the discrete Markov analysis is utilized to estimate the varieties of twist in the area as in [24] The speed of the wind states is counted by the ramifications of discrete Markov analysis as abridged in Table 1 and probability density function supported picture as in Figure 1. Facilitate the above examined technique is fused to find the probability of the WES control as appeared in Figure 2 and specified in Table 2.

Objective Function

The intention of this investigation is to allocate the ESS optimally by PSO, to capture the surplus power produced by the WES and enhance voltage profile of the assumed IEEE 30 bus test system by way of [25] as observed in Figure 3 and a new demonstration of IEEE 57 bus system. However, the focal of the study to curtail the whole expenses of power system perhaps the proposed algorithm PSO must satisfy the enumerated constraints for the appropriate functioning power system. The goal of this examination is to assign the ESS ideally by PSO, to catch the surplus power created by the WES and upgrade voltage profile of the expected IEEE 30 transport test system by method for [25] IEEE 57 bus system. Be that as it may, the central of the investigation to reduce the entire costs of power system maybe the proposed calculation PSO must fulfill the identified imperatives for the proper working power system. The scope of the functions is characterized to two objectives and is composed as follows,

Reduction in expenditure of the test systems:

The minimization of overall expenses is modeled as

$$\min R1 = \sum_{k=1}^5 O_k T_k$$

Where the O_k is the operation cost probability at the consideration of k . The overall expenditure cost of the operation in (\$/h) through k described by , further the E_k is detailed as equation 2

$$T_k = T(P_{gt}) + T_w + T_{ess}$$

In the demonstration of (P_{gt}) is induced generators task cost (\$/h), WES working expense is spoken to by T_w (\$/h) and T_{ess} shows the cost of energy storage system (\$/h). Each term in the above articulation is advised as

The general costs of the conventional generator are expressed by

$$T(P_{gt}) = \sum_{t=1}^g (a'_f + b'_f (P_{gt}) + c'_f (P_{gt})^2)$$

Wherever a'_f, b'_f, c'_f are fuel coefficient of generator f and entire number of generators is represented by g .

The expenditure incurred by the WES is contemplated by

$$T_w = t_w^{o.c} \cdot P_w$$

As $t_w^{o.c}$ is WES functioning cost and power is produced by the wind is indicated by P_w .

The cost for the functioning of energy storage system as

$$T_{ess} = t_{ess}^{o.c} \cdot P_{capacity}$$

Where $t_{ess}^{o.c}$ intimating the expenses of ESS and $P_{capacity}$ is established capacity of ESS.

Progression of Voltage outline

The voltage profile headway of assumed test bus system is exhibited as,

$$\min F2 = \sum_{x=1}^m \left(\frac{B - B_{exp}}{\Delta B^{max}} \right)^2$$

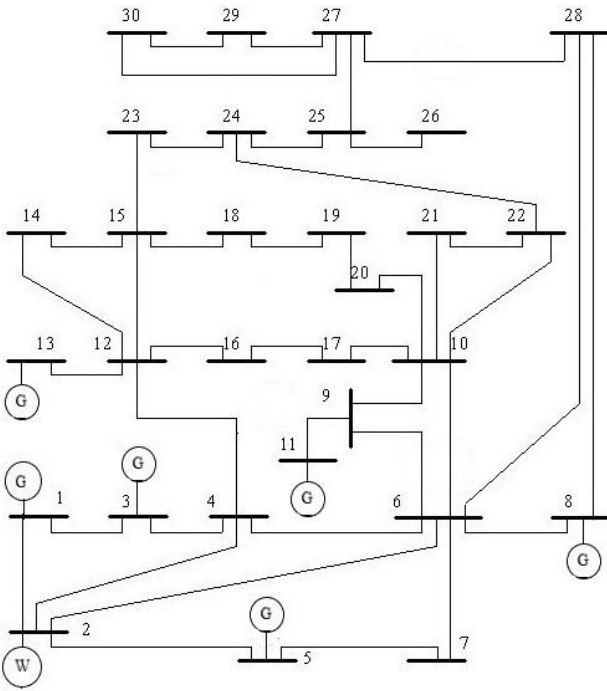
Where m is the whole include of transports the stepped through examination system. The normal voltage in the grid is communicated by . The maximum in change of voltage is indicated by ΔB_{max} , anyway needs to fulfill the power stream limitations as in [23] and to achieve the restrictions in voltages in transport and transformer taps and created reactive power as portrayed in following limits individually.

$$\begin{aligned} B_m &\leq B_k \leq B_M \\ T_m &\leq T_k \leq T_M \\ Q_{Gm} &\leq Q_k \leq Q_{GM} \end{aligned}$$

As B_k is voltages in the bus k , T_k is taps in the transformer k and Q_k is hinting reactive power of the generator k .

Particle swarm optimization and implementation

The principle behind the PSO is to produce populace of swarms made out of colossal particles as of [1,2&5]. Every molecule is established to the errand of settling the advancement inconvenience by familiarize with idle arrangement in dimensional investigation bound of O inside the populace R . The best spot of the particle is restored in view of its swarm broad association.



The velocity vector is attested by

$$\begin{aligned} A_m^{z+1} &= A_m^z + h_m^{z+1} \\ h_m^{z+1} &= S h_m^z + c_1 t_1 + (n_m^z - a_m^z) + c_2 t_2 (v_m^z - a_m^z) \\ n_m^z &= [a_{m1}^n, y_{m2}^n, \dots, y_{m0}^n] \\ v_m^z &= [a_{m1}^w, a_{m2}^w, \dots, a_{m0}^w] \end{aligned}$$

As s is inertia weight, c_1 and c_2 are acceleration constants, t_1 and t_2 are random numbers in the bound of $[0,1]$, n_m^z is best spot of particle m and a_m^z Swarm experience-based

particle position. The efficacy of the projected method is improved by

$$S^z = S_o - \left(\frac{S_o - S_m}{S_o} \right)$$

Where S_M is introductory inertia weight and last inertia weight is S_m . The maximum cycle number is Z_o .

Implementation of PSO

The proposed PSO model is affected in presumed IEEE 30 transport test system as Figure 3 and adjusted IEEE 57 transport system as aftereffect of rehashing the information in 30 transport system for the itemized examination of PSO for the optimal allocation of ESS. The vitality produced from this WES has been classified into five levels as marked in Table 2. The interest for the picked test system of IEEE depends on [23] and it has been multiplied for altered IEEE 57 bus system.

Conformation of IEEE 30 bus system

The evaluation arrangement of IEEE 30 bus system is designed with the end goal that qualification of twenty loads and five number of thermal power generators typified as G have been related to accepted framework at PV transports of 5, 8, 11 and 13. Not with standing that transport 1 bordered with warm plant as G turned as slack transport and lingering buses are locked in as PQ transport as in [25]. The WES has been consolidated to bus 2 and spoke to as W in Figure 3 with the volume of 113 MW.

Conformation of modified IEEE 57 bus system

The evaluation arrangement of IEEE 57 transport framework is designed with the end goal that privilege of forty burdens and seven number of warm power generators encapsulated as G have been related to expected framework at PV transports of 5, 8, 10, 11, 13, 16 and 22. In addition to that bus 1 adjoined with thermal plant as G turned as slack bus and residual buses are engaged as PQ bus. The WES has been combined to buses 2 and 4 represented as W in Fig 3 with the volume of 226 MW. The arranged model of PSO is actualized as takes after

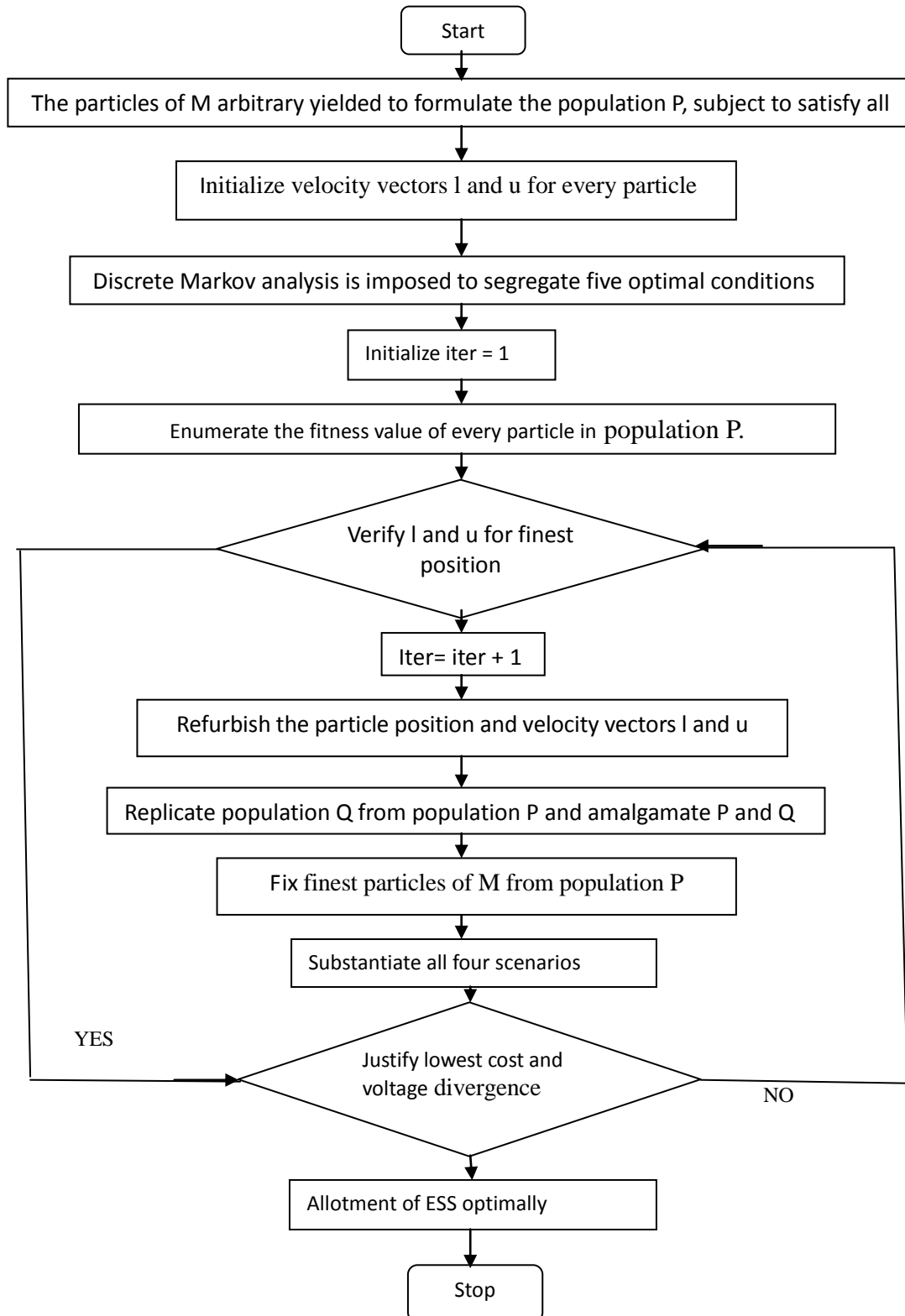
- Step 1: The particles of M arbitrary yielded to formulate population P , subject to satisfy all constraints.
- Step 2: Initialize velocity vectors l and u for every particle.
- Step 3: Discrete Markov analysis is imposed to segregate five optimal conditions.
- Step 4: Enumerate the fitness value of every particle in population P .
- Step 5: Verify l and u for finest position.
- Step 6: Shift to step 11 or else move to next step.
- Step 7: Iteration = Iteration + 1.
- Step 8: Refurbish the particle position and velocity vectors l and u .
- Step 9: Replicate population Q from population P and amalgamate P and Q .
- Step 10: Fix the finest particles of M from population P .

Step 11: Substantiate all four scenarios and validate lowest expenditure and voltage divergence if criteria is not satisfied move to step 7.

Step 13: Allotment of ESS optimally.

Step 14: Stop.

The flowchart of the proposed algorithm is shown in Fig 1.



In this case, OPF is connected to examination test, the genuine power misfortune has been bit by bit declining when the wind power is admitted to the system continuously as in Table 7. Simultaneously, the activity cost of the examination system has been decreasing as summarized in Table 6. The voltage profile for this assumed test system is advised in Table 3.

Circuit Modelling of UPQC

The control system consists of three major elements, which are shunt inverter control, series inverter control, and DC/DC converter control. When the level of the source voltage is maintained at 1.0 p.u., the system works in normal mode. When the level falls between 0.5 and 1.0 p.u. or higher than 1.0 p.u., the system works in voltage sag or swell mode. When the level is lower than 0.5 p.u., the system works in interruption mode. In normal mode, the series inverter injects the zero voltage and the shunt inverter absorbs the current harmonics generated by the load. The DC/DC converter works in charge mode or standby mode depending on the voltage level of the super capacitors.

In voltage hang o swell mode, the arrangements inverter infuses the replaying voltage to keep up the heap voltage steady. The shunt inverter retains the present sounds produced by the heap and the DC/DC converter works in standby mode. In voltage interruption mode, the series inverter is disconnected from the line and the circuit breaker is opened to isolate the source side. The shunt inverter starts to work as an AC voltage source. The DC/DC converter works in discharge mode to supply the energy stored in the super-capacitors to the

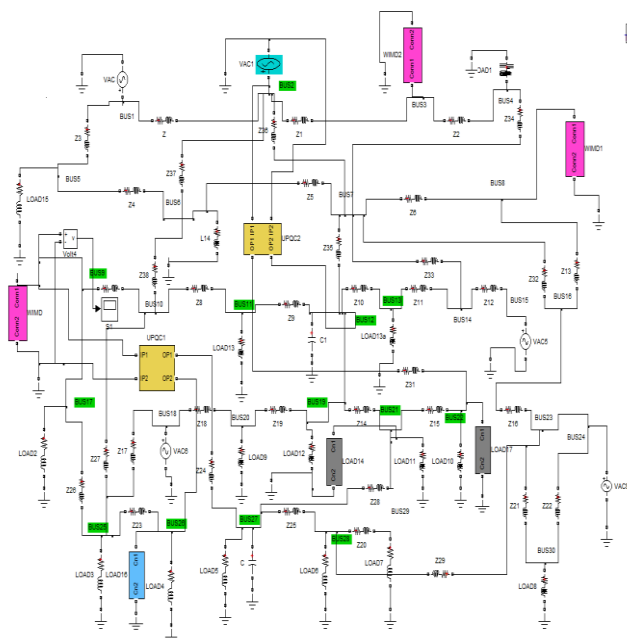
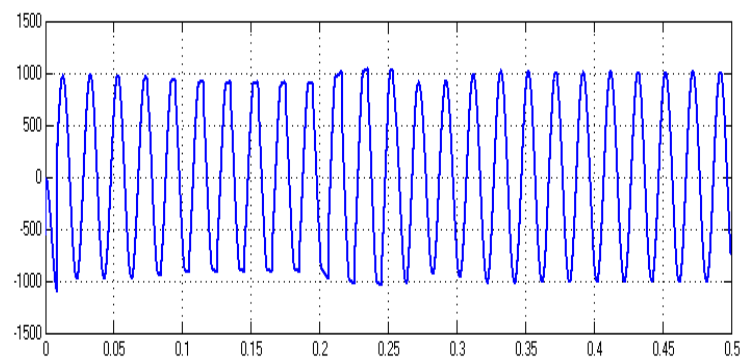
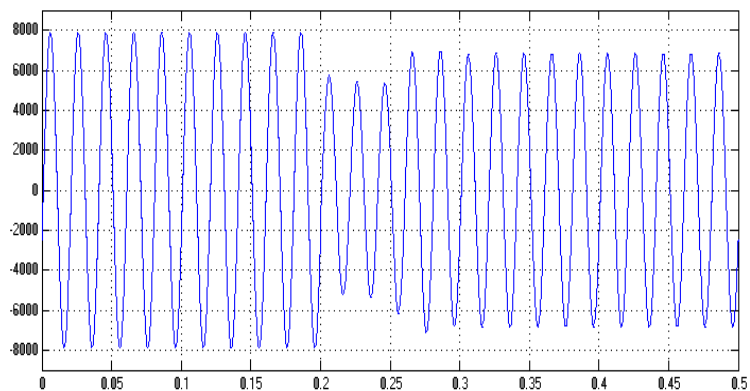


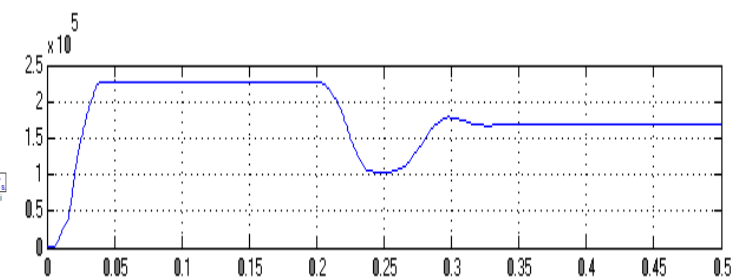
Fig.2 30 -bus system with Wind Power Distribution for With Facts



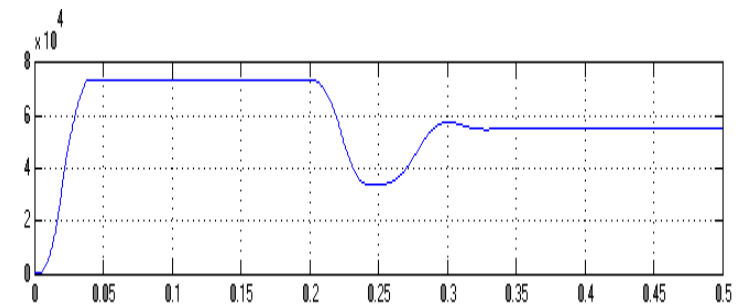
Wind output voltage



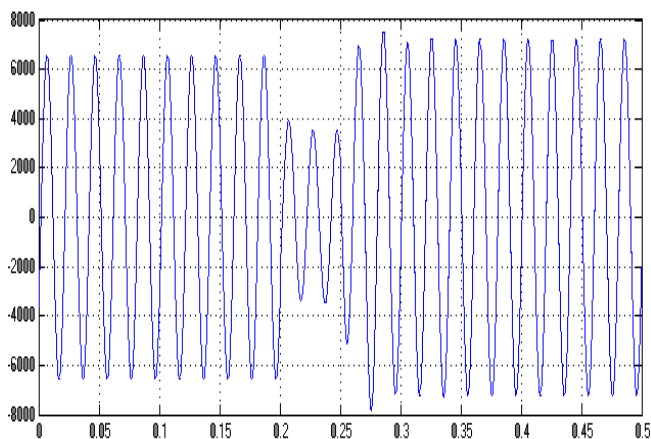
BUS-4 VOLTAGE



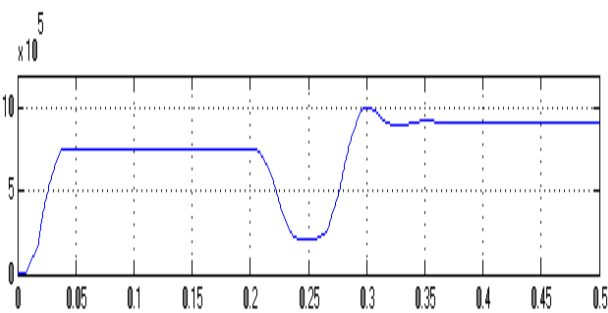
REAL POWER AT BUS 4



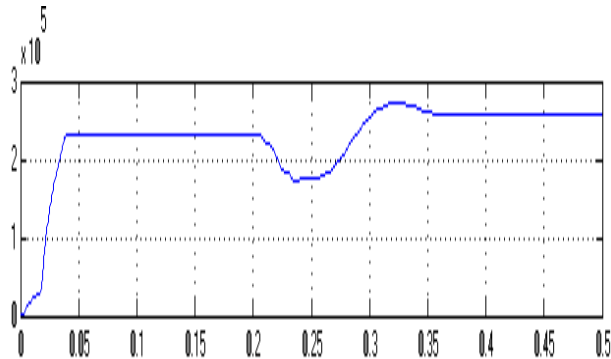
REACTIVE POWER AT BUS 4



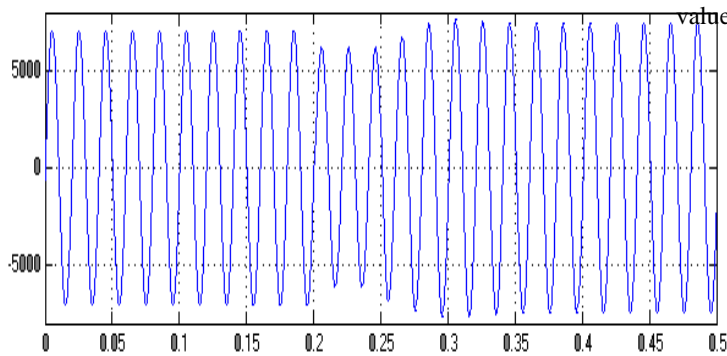
BUS-12 VOLTAGE



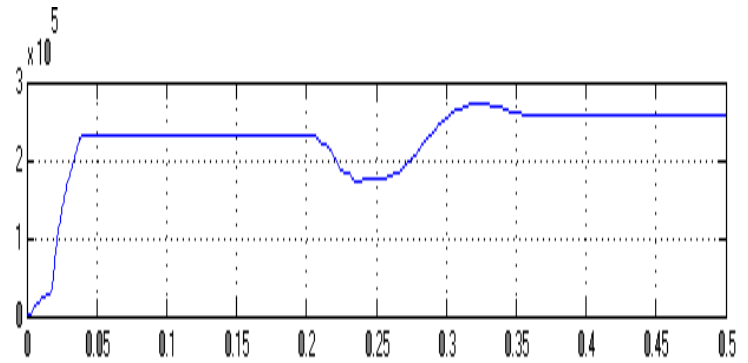
REAL POWER AT BUS 12



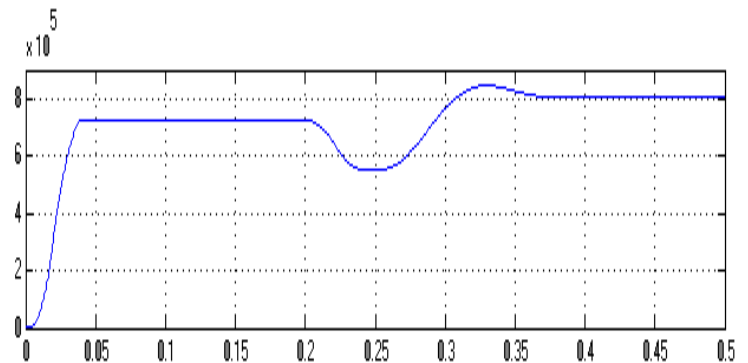
REACTIVE POWER AT BUS 12



BUS-26 VOLTAGE



REAL POWER AT BUS 26



REACTIVE POWER AT BUS 26

Thirty-Bus System for Wind Power Distribution without FACTS

The Real power at bus-4 is shown in Fig.4.4 and its value is 1.5×10^5 watts. The Reactive power at bus-4 is shown in Fig.4.5 and its value is 4.5×10^4 watts. The voltage of the 12-bus system is shown in Fig.4.6 and its peak value is 0.85×10^4 V.

The real power at bus-12 is shown in Fig.4.7 and its value is 6.4×10^5 watts. The reactive power at bus-12 is shown in Fig.4.8 and its value is 2.4×10^5 watts. The voltage of the 26-bus system is shown in Fig.4.9 and its peak value is 8000 V.

The real power at bus-26 is shown in Fig.4.10 and its value is 2.25×10^5 watts.

The reactive power at bus-26 is shown in Fig.4.11 and its value is 6.9×10^5 watts.

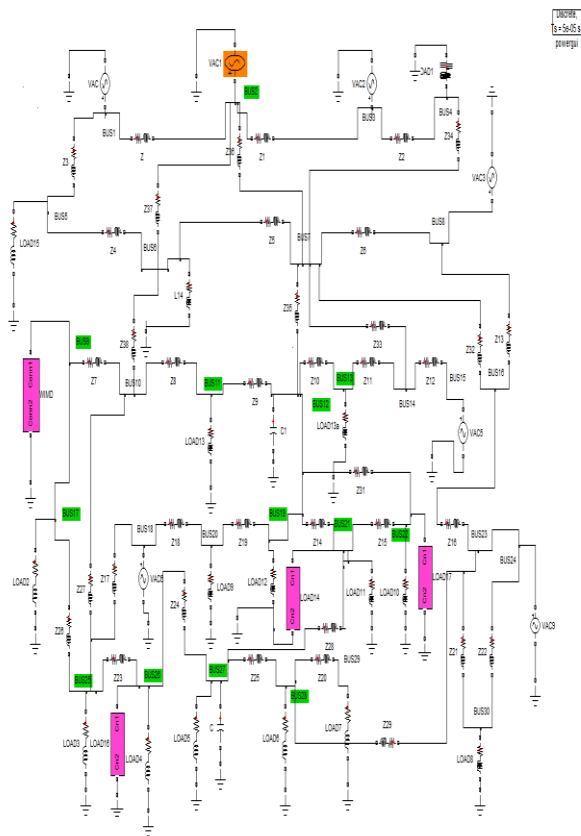
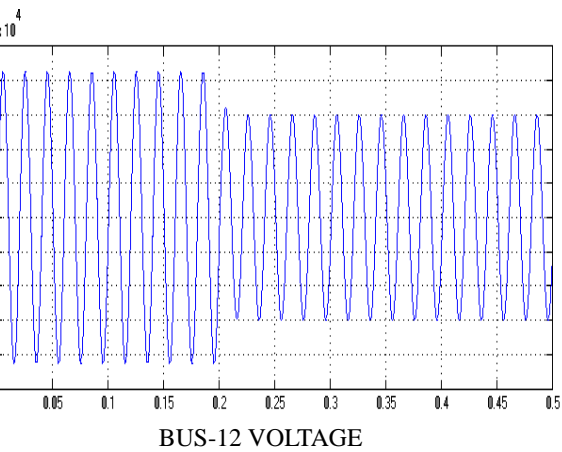
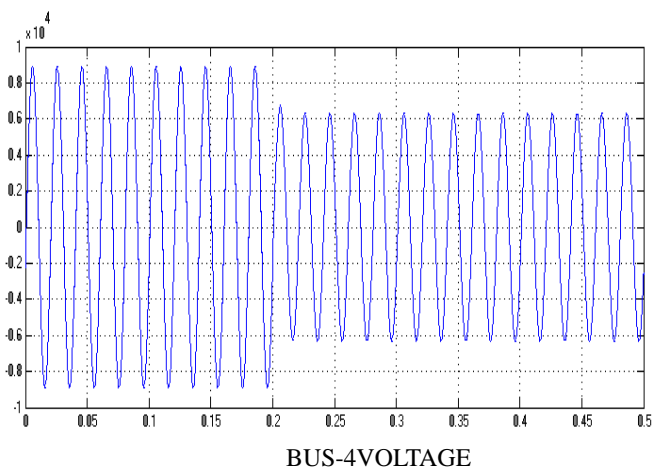
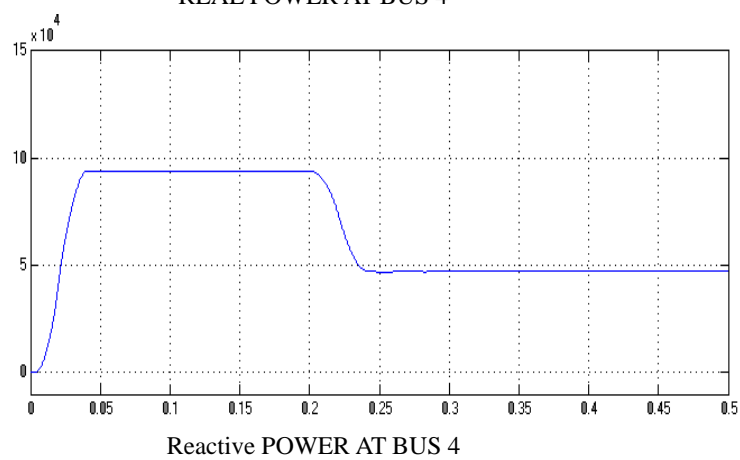
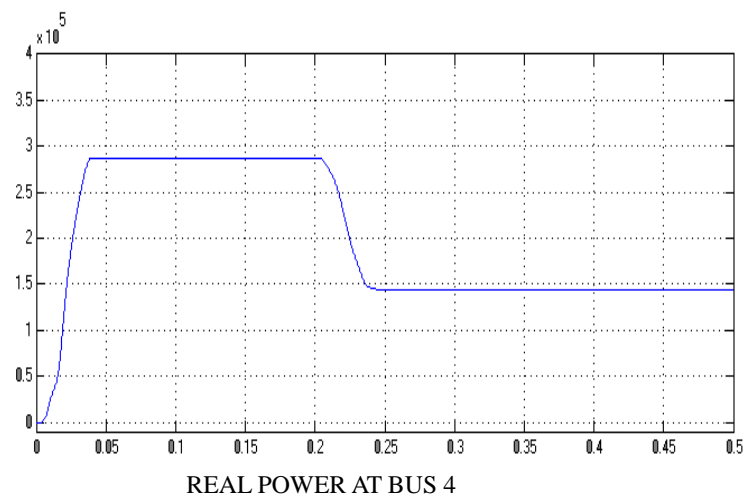
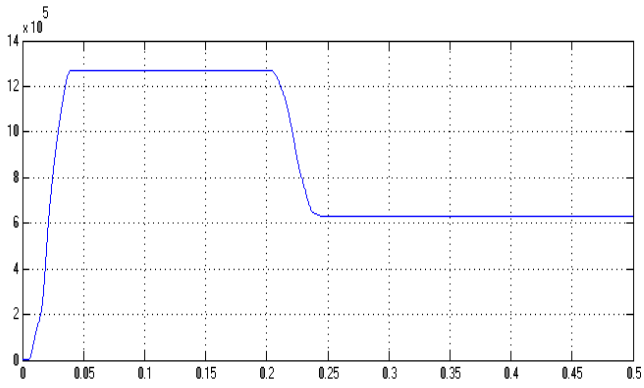
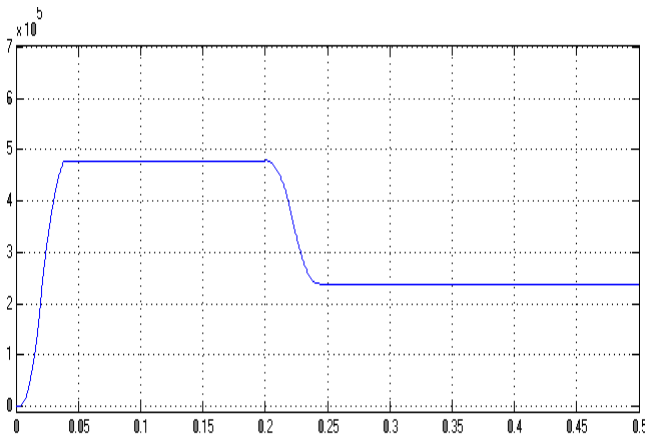


Fig.3 30- bus system with Wind Power Distribution for without Facts

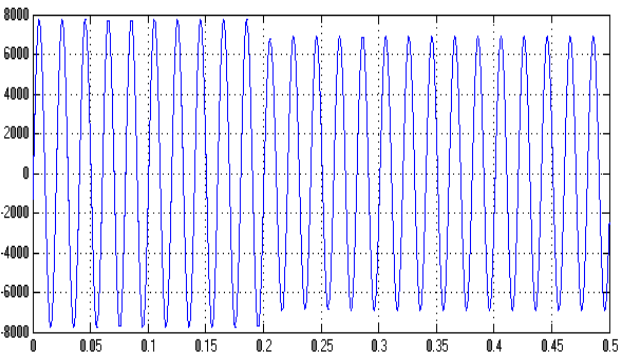




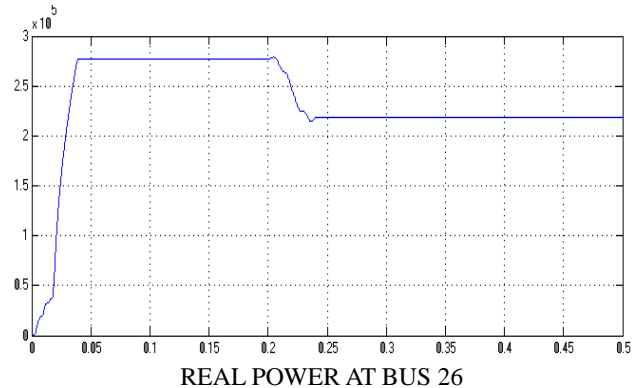
REAL POWER AT BUS 12



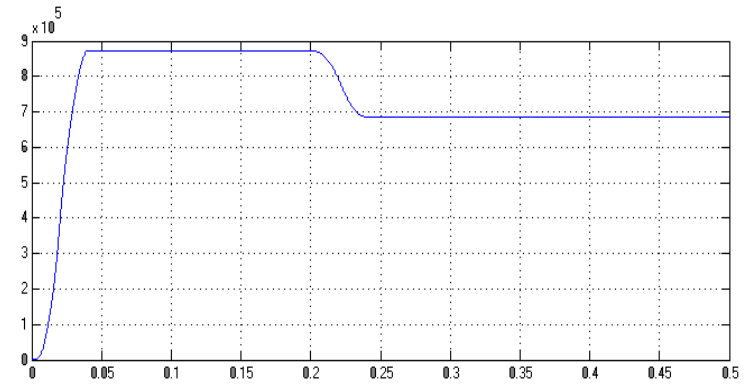
Reactive POWER AT BUS 12



BUS-26VOLTAGE



REAL POWER AT BUS 26



Reactive POWER AT BUS 26

Consequences and deliberation

In this effort, two plans have been inspected practically equivalent to evaluation framework united WES and test framework coordinate with mix of WES and ESS. The OPF (ideal power stream) technique and anticipated strategy PSO are connected over the above proclaimed cases for corresponded thought and nitty gritty as takes after.

Comparison of real and reactive power:

Bus no	P (MW) without Facts	P (MW) with Facts	Q (MVAR) without Facts	Q (MVAR) With Facts
4	0.149	0.163	0.049	0.051
5	0.138	0.152	0.091	0.113
6	0.126	0.149	0.106	0.118
7	0.123	0.145	0.103	0.114
8	0.146	0.161	0.098	0.104
10	0.153	0.190	0.099	0.101
11	0.367	0.360	0.109	0.113
12	0.356	0.423	0.108	0.150
13	0.294	0.356	0.122	0.138
15	0.286	0.345	0.128	0.146
16	0.281	0.338	0.118	0.136

17	0.279	0.334	0.114	0.128
19	0.277	0.327	0.108	0.105
20	0.198	0.229	0.081	0.096
21	0.144	0.169	0.047	0.055
22	0.632	0.717	0.337	0.446
23	0.548	0.614	0.281	0.326
25	0.364	0.377	1.14	1.185
26	0.218	0.257	0.685	0.807
27	0.210	0.248	0.523	0.568
28	0.221	0.263	0.256	0.276
30	0.239	0.274	0.228	0.254

Analysis of IEEE 30 bus system

Application of OPF

In this case, OPF is applied to analysis test system, the real power loss has been gradually declining when the wind power is admitted to the system progressively as in Table 7. Simultaneously, the operation cost of the appraisal system has

been decreasing as summarized in Table 6. The voltage profile for this assumed test system is briefed in Table 3.

IEEE 30 bus system integrated WES

WIND POWER	0 (MW)	14.54 (MW)	55.79 (MW)	98.12 (MW)	113 (MW)
BUS	Voltage (p.u)	Voltage (p.u)	Voltage (p.u)	Voltage (p.u)	Voltage (p.u)
1	1.06	1.06	1.06	1.06	1.06
2	1.045	1.045	1.045	1.045	1.045
3	1.012	1.012	1.013	1.014	1.015
4	1.007	1.008	1.008	1.009	1.01
5	1.01	1.01	1.01	1.01	1.02
6	1.009	1.009	1.009	1.009	1.009
7	1.001	1.001	1.002	1.002	1.002
8	1.01	1.01	1.01	1.01	1.01
9	1.05	1.05	1.05	1.05	1.05
10	1.044	1.044	1.044	1.044	1.044
11	1.082	1.082	1.082	1.082	1.082
12	1.055	1.056	1.056	1.057	1.057
13	1.071	1.071	1.071	1.072	1.072
14	1.041	1.041	1.041	1.041	1.041
15	1.036	1.036	1.036	1.037	1.037
16	1.043	1.043	1.043	1.043	1.044
17	1.039	1.039	1.039	1.039	1.039
18	1.027	1.027	1.027	1.027	1.027
19	1.024	1.024	1.025	1.025	1.025
20	1.028	1.028	1.029	1.029	1.029
21	1.031	1.032	1.032	1.032	1.032
22	1.032	1.032	1.033	1.033	1.033
23	1.026	1.026	1.026	1.026	1.026
24	1.020	1.02	1.021	1.021	1.021
25	1.016	1.016	1.016	1.017	1.017
26	0.998	0.998	0.999	0.999	0.999
27	1.022	1.022	1.022	1.023	1.023
28	1.006	1.006	1.007	1.008	1.006

29	1.002	1.002	1.003	1.004	1.004
30	0.991	0.991	0.992	0.992	0.993

Table 3. Voltage outline for IEEE 30 bus system with WES

IEEE 30 bus system combined with WES and ESS

In this exertion, ESS has been coupled and the area for the acceptance of the ESS has been characterized by the OPF as précised in Table 4. The whole size of ESS is 43.2 MW. The

connection of ESS has occasioned to diminishing the activity cost and also genuine power loss of the test system accepted as explained in Table 7. The extent of voltage in each clean is shown in Table 4.

OPF					
WIND POWER	0 (MW)	14.54 (MW)	55.79 (MW)	98.12 (MW)	113 (MW)
BUS	Voltage (p.u)	Voltage (p.u)	Voltage (p.u)	Voltage (p.u)	Voltage (p.u)
1	1.06	1.06	1.06	1.06	1.06
2	1.045	1.045	1.045	1.045	1.045
3	1.012	1.034	1.035	1.036	1.036
4	1.007	1.031	1.032	1.032	1.032
5	1.01	0.985	0.985	0.986	0.986
6	1.009	1.032	1.033	1.033	1.033
7	1.001	1.005	1.006	1.006	1.006
8	1.01	1.02	1.021	1.021	1.021
9	1.05	1.091	1.091	1.092	1.092
10	1.044	1.11	1.111	1.111	1.111
11	1.082	1.091	1.091	1.092	1.092
12	1.055	1.102	1.103	1.104	1.104
13	1.071	1.102	1.103	1.104	1.104
14	1.041	1.098	1.098	1.099	1.099
15	1.036	1.103	1.104	1.104	1.104
16	1.043	1.099	1.099	1.100	1.100
17	1.039	1.102	1.103	1.103	1.103
18	1.027	1.133	1.134	1.134	1.135
19	1.024	1.154	1.155	1.155	1.155
20	1.028	1.142	1.143	1.144	1.144
21	1.031	1.104	1.105	1.106	1.106
22	1.032	1.107	1.108	1.108	1.108
23	1.026	1.093	1.094	1.095	1.095
24	1.02	1.089	1.089	1.09	1.09
25	1.016	1.07	1.071	1.071	1.071
26	0.998	1.053	1.054	1.055	1.055
27	1.022	1.067	1.067	1.068	1.068
28	1.006	1.035	1.036	1.036	1.036
29	1.002	1.048	1.049	1.049	1.049
30	0.991	1.037	1.038	1.038	1.038
Allocation of ESS	Bus 6/2.5MW, Bus 19/18.2MW, Bus 22/5.6MW, Bus 28/16MW				
Total size of ESS	43.2 MW				

Table 4. Voltage outline for IEEE 30 bus system with WES allied ESS

Implementation of PSO**WES allied IEEE 30 bus system**

The PSO has been executed to examination system, the real power misfortune has been drastically decreased contrasted with the symmetry condition to the utilization of OPF. As of the Table 8 misfortune in real power is

12.5061 MW, while the commitment from The purposed calculation PSO actualized to consequent investigations as the wind is 113 MW in this express the working expense of the system is \$ 9498.7/hour. The voltage profile of the buses is outstanding around the estimation of 1.01 pu as revealed in Table 5

PSO					
WIND POWER	0 (MW)	14.54 (MW)	55.79 (MW)	98.12 (MW)	113 (MW)
BUS	Voltage (p.u)	Voltage (p.u)	Voltage (p.u)	Voltage (p.u)	Voltage (p.u)
1	1.06	1.06	1.06	1.06	1.06
2	1.045	1.045	1.045	1.045	1.045
3	1.0191	1.0198	1.0185	1.0192	1.0205
4	1.0138	1.0146	1.0142	1.0140	1.0154
5	1.01	1.01	1.01	1.01	1.01
6	1.0126	1.0127	1.0128	1.0133	1.0134
7	1.0036	1.0037	1.0038	1.0041	1.0041
8	1.01	1.01	1.01	1.01	1.01
9	1.0528	1.0529	1.0529	1.0529	1.0532
10	1.0472	1.0476	1.0477	1.0479	1.0488
11	1.0820	1.0820	1.0820	1.0820	1.0820
12	1.0605	1.0589	1.0588	1.0588	1.0588
13	1.0710	1.0710	1.0710	1.0710	1.0710
14	1.0438	1.0441	1.0441	1.0441	1.0457
15	1.0392	1.0396	1.0397	1.0399	1.0405
16	1.0459	1.0468	1.0465	1.0467	1.0473
17	1.0415	1.0422	1.0425	1.0425	1.0432
18	1.0297	1.0303	1.0304	1.0307	1.0309
19	1.0272	1.0281	1.0283	1.0287	1.0297
20	1.0313	1.0330	1.0322	1.0321	1.0330
21	1.0348	1.0352	1.0353	1.0354	1.0363
22	1.0353	1.0357	1.0358	1.0359	1.0367
23	1.0286	1.0286	1.0295	1.0295	1.0296
24	1.0229	1.0235	1.0236	1.0236	1.0240
25	1.0179	1.0182	1.0184	1.0184	1.0184
26	1.0002	1.0005	1.0007	1.0008	1.0008
27	1.0231	1.0236	1.0238	1.0238	1.0238
28	1.0087	1.0087	1.0087	1.0087	1.0093
29	1.0032	1.0038	1.0039	1.004	1.0041
30	0.9917	0.9923	0.9925	0.9925	0.9925

Table 5. Voltage outline for IEEE 30 bus system with WES

WES and ESS associated IEEE 30 bus system

In this specific circumstance, the PSO has been inspected over the assessed test system with the osmosis of ESS. The PSO has separated the situation of ESS with regards to the buses 7, 16 and 30 correspondingly. The whole limit of ESS associated is 29.2 MW as indicated in Table 6. In the test system, vigorous voltage diagram has been seen according to Table 8. The span of ESS joined in the midst of the execution by OPF is slighter than execution by PSO, regardless the activity cost of test framework in PSO is temperate of \$ 9512.20/hour versus \$ 9832.41/hour in OPF for the zero

penetration of the WES control. In PSO if the whole intensity of WES infused to the system the costs is \$ 9498.70/hour against \$ 9509.77/hour for OPF as saw in the Tables 7 and 8 separately. Haphazardly translating the pa swarm improvement against its partner OPF for the investigation of WES, its consumption are \$ 9740.26/hour and \$ 9502.50/hour separately as inspired in Figure 4. Another investigation of same case ESS joined WES the cost is \$9758.72/ticle for OPF versus \$9502.70/hour for PSO as portrayed in Figure 5.

PSO					
WIND POWER	0 (MW)	14.54 (MW)	55.79 (MW)	98.12 (MW)	113 (MW)
BUS	Voltage (p.u)	Voltage (p.u)	Voltage (p.u)	Voltage (p.u)	Voltage (p.u)
1	1.06	1.06	1.06	1.06	1.06
2	1.045	1.045	1.045	1.045	1.045
3	1.0458	1.0457	1.0457	1.0460	1.0464
4	1.0435	1.0435	1.0435	1.0438	1.0442
5	0.9928	0.9927	0.9927	0.9929	0.9931
6	1.0474	1.0471	1.0472	1.0475	1.0479
7	1.0175	1.0173	1.0173	1.0176	1.0179
8	1.0358	1.0355	1.0355	1.0359	1.0365
9	1.1084	1.1077	1.1078	1.1088	1.1089
10	1.1286	1.1276	1.1278	1.1290	1.1290
11	1.1084	1.1077	1.1078	1.1088	1.1089
12	1.1162	1.1168	1.1167	1.1165	1.1176
13	1.1162	1.1168	1.1167	1.1165	1.1176
14	1.1116	1.1125	1.1124	1.1120	1.1134
15	1.1173	1.1189	1.1186	1.1180	1.1200
16	1.1151	1.1148	1.1149	1.1155	1.1159
17	1.1195	1.1188	1.1189	1.1199	1.1201
18	1.1454	1.1502	1.1492	1.1470	1.1516
19	1.1649	1.1716	1.1701	1.1669	1.1731
20	1.1552	1.1600	1.1589	1.1569	1.1615
21	1.1269	1.1238	1.1243	1.1274	1.1258
22	1.1305	1.1267	1.1274	1.1210	1.1289
23	1.1101	1.1103	1.1102	1.1107	1.1118
24	1.1082	1.1066	1.1068	1.1086	1.1085
25	1.0870	1.0863	1.0864	1.0872	1.0885
26	1.0705	1.0697	1.0699	1.0707	1.0720
27	1.0819	1.0817	1.0818	1.0820	1.0841
28	1.0501	1.0497	1.0498	1.0502	1.0521
29	1.0633	1.0631	1.0631	1.0633	1.0654
30	1.0525	1.0523	1.0523	1.0525	1.0547
Allocation of ESS	Bus 7/12.1 MW, Bus 16/9.7 MW and Bus 30/7.4 MW				
Capacity of ESS	29.2 MW				

Table 6. Voltage outline for IEEE 30 bus system with WES allied ESS

Wind Power (MW)	OPF			
	Total Real power loss (MW)		Operation Cost (\$/hr)	
	Exclusion of ESS	Inclusion of ESS	Exclusion of ESS	Inclusion of ESS
0	27.447	19.966	9815.93	9832.41
14.54	25.402	18.356	9740.26	9758.72
55.79	20.480	14.433	9574.06	9758.72
98.12	16.714	11.970	9477.65	9521.28
113	15.685	11.319	9458.60	9509.77

Table 7. Total real power loss and operation cost for IEEE 30 bus system

Wind Power (MW)	PSO			
	Total Real power loss (MW)		Operation Cost (\$/hr)	
	Exclusion of ESS	Inclusion of ESS	Exclusion of ESS	Inclusion of ESS
0	14.530	12.663	9509.10	9512.20
14.54	14.514	12.531	9502.50	9502.70
55.79	14.503	12.532	9500.10	9502.50
98.12	14.498	12.502	9498.90	9498.80
113	14.266	12.506	9498.70	9498.70

Table 8. Total real power loss and operation cost for IEEE 30 bus system

5.1 Analysis of altered IEEE 57 bus system:

5.1.1 Application of OPF

The OPF applied to succeeding cases as

i. Altered IEEE 57 bus system integrated WES

In this case, OPF is applied to analysis test system, the real power loss has been gradually declining when the wind power is admitted to the system progressively as in Table 14. Simultaneously, the operation cost of the appraisal system has been decreasing as summarized in Table 13. The voltage profile for this assumed test system is briefed in Table 9.

OPF					
WIND POWER	0 (MW)	14.54 (MW)	55.79 (MW)	98.12 (MW)	113 (MW)
BUS	Voltage (p.u)	Voltage (p.u)	Voltage (p.u)	Voltage (p.u)	Voltage (p.u)
1	1.04	1.04	1.04	1.04	1.04
2	1.01	1.01	1.01	1.01	1.01
3	0.985	0.985	0.985	0.985	0.985
4	0.981	0.981	0.981	0.981	0.981
5	0.977	0.977	0.976	0.977	0.977
6	0.980	0.980	0.980	0.981	0.981
7	0.984	0.984	0.984	0.985	0.985
8	1.005	1.005	1.005	1.006	1.006
9	0.980	0.980	0.980	0.981	0.981
10	0.986	0.986	0.986	0.986	0.986
11	0.974	0.974	0.974	0.974	0.975
12	1.015	1.015	1.015	1.015	1.016
13	0.979	0.979	0.979	0.979	0.980
14	0.970	0.970	0.970	0.970	0.971
15	0.988	0.988	0.988	0.988	0.988
16	1.013	1.013	1.013	1.014	1.014
17	1.017	1.017	1.018	1.018	1.018
18	1.000	1.000	1.001	1.002	1.002
19	0.971	0.971	0.970	0.969	0.969
20	0.965	0.965	0.964	0.962	0.962
21	1.008	1.008	1.009	1.009	1.009
22	1.010	1.010	1.011	1.011	1.011
23	1.008	1.008	1.009	1.009	1.009
24	0.999	0.999	1.000	1.000	1.000
25	0.982	0.982	0.983	0.983	0.983
26	0.959	0.959	0.960	0.960	0.960
27	0.981	0.981	0.982	0.983	0.983
28	0.996	0.996	0.997	0.998	0.998
29	1.010	1.010	1.010	1.011	1.011
30	0.963	0.963	0.964	0.965	0.965
31	0.936	0.936	0.937	0.937	0.937
32	0.950	0.950	0.951	0.952	0.952
33	0.947	0.948	0.949	0.949	0.949
34	0.959	0.959	0.959	0.959	0.959
35	0.966	0.966	0.967	0.968	0.968
36	0.976	0.976	0.977	0.978	0.978
37	0.985	0.985	0.985	0.986	0.986
38	1.013	1.013	1.014	1.015	1.015
39	0.983	0.983	0.984	0.985	0.985
40	0.973	0.973	0.974	0.974	0.974
41	0.996	0.996	0.996	0.997	0.997
42	0.967	0.967	0.968	0.968	0.968
43	1.010	1.010	1.02	1.02	1.02

44	1.017	1.017	1.018	1.018	1.018
45	1.036	1.036	1.036	1.037	1.037
46	1.060	1.060	1.061	1.061	1.061
47	1.033	1.033	1.034	1.034	1.034
48	1.027	1.027	1.028	1.028	1.028
49	1.036	1.036	1.036	1.037	1.037
50	1.024	1.023	1.024	1.024	1.024
51	1.053	1.052	1.053	1.053	1.053
52	0.980	0.980	0.981	0.982	0.982
53	0.971	0.971	0.972	0.973	0.973
54	0.996	0.996	0.997	0.998	0.998
55	1.031	1.031	1.032	1.032	1.032
56	0.968	0.968	0.969	0.969	0.969
57	0.965	0.965	0.965	0.965	0.965

Table 9. Voltage outline for altered IEEE 57 bus system with WES

Altered IEEE 57 bus system integrated combined with WES and ESS

In this effort, ESS has been coupled and the location for the induction of the ESS has been defined by the OPF as précised in Table 10. The entire magnitude of ESS is 86.4 MW. The attachment of ESS has occasioned to lessening the operation cost as well as real power loss of the test system assumed as elaborated in Table 13. The magnitude of voltage in each bus is indicated in Table 10.

OPF					
WIND POWER	0 (MW)	14.54 (MW)	55.79 (MW)	98.12 (MW)	113 (MW)
BUS	Voltage (p.u)	Voltage (p.u)	Voltage (p.u)	Voltage (p.u)	Voltage (p.u)
1	1.009	1.011	1.009	1.01	1.01
2	1.010	1.012	1.010	1.012	1.011
3	1.002	1.000	1.003	1.007	1.009
4	1.006	1.005	1.007	1.009	1.010
5	1.016	1.017	1.016	1.015	1.015
6	1.026	1.028	1.026	1.024	1.023
7	1.025	1.026	1.025	1.022	1.021
8	1.045	1.045	1.044	1.041	1.040
9	1.005	1.005	1.004	1.002	1.002
10	0.985	0.985	0.984	0.983	0.983
11	0.984	0.985	0.984	0.983	0.983
12	0.992	0.993	0.992	0.991	0.990
13	0.978	0.978	0.978	0.977	0.977
14	0.970	0.970	0.970	0.970	0.970
15	0.988	0.988	0.988	0.989	0.989
16	0.991	0.992	0.991	0.990	0.990

17	0.993	0.994	0.993	0.992	0.992
18	1.026	1.024	1.026	1.029	1.030
19	0.988	0.988	0.988	0.989	0.990
20	0.977	0.977	0.977	0.977	0.977
21	1.015	1.015	1.015	1.015	1.015
22	1.015	1.015	1.015	1.015	1.015
23	1.014	1.014	1.014	1.014	1.014
24	1.017	1.018	1.017	1.016	1.016
25	1.001	1.001	1.001	1.000	1.000
26	0.976	0.977	0.976	0.975	0.975
27	1.013	1.014	1.013	1.011	1.011
28	1.034	1.035	1.003	1.031	1.031
29	1.051	1.052	1.050	1.048	1.047
30	0.980	0.981	0.980	0.979	0.979
31	0.951	0.951	0.951	0.950	0.950
32	0.960	0.960	0.960	0.960	0.959
33	0.958	0.958	0.958	0.957	0.957
34	0.967	0.967	0.967	0.966	0.966
35	0.973	0.973	0.973	0.973	0.973
36	0.982	0.983	0.982	0.982	0.982
37	0.991	0.991	0.991	0.990	0.990
38	1.016	1.016	1.016	1.016	1.016
39	0.989	0.989	0.989	0.988	0.988
40	0.980	0.980	0.980	0.979	0.979
41	1.007	1.007	1.007	1.006	1.005
42	0.975	0.975	0.975	0.974	0.974
43	1.020	1.021	1.020	1.019	1.018
44	1.019	1.019	1.019	1.019	1.019
45	1.035	1.034	1.035	1.036	1.036
46	1.060	1.060	1.060	1.060	1.060
47	1.034	1.034	1.034	1.034	1.034
48	1.029	1.029	1.029	1.029	1.029
49	1.038	1.038	1.038	1.037	1.037
50	1.024	1.025	1.024	1.023	1.023
51	1.052	1.053	1.052	1.050	1.050
52	1.020	1.021	1.019	1.017	1.016
53	1.01	1.011	1.009	1.007	1.006
54	1.03	1.031	1.029	1.027	1.026
55	1.04	1.060	1.059	1.056	1.055
56	0.975	0.975	0.975	0.974	0.974
57	0.970	0.970	0.971	0.970	0.969
Allocation of ESS	Bus 6/5 MW, Bus 8/36.4 MW, Bus 9/11.2 MW, Bus12 /32 MW				
Total size of ESS	86.4 MW				

Table 10. Voltage outline for altered IEEE 57 bus system with WES allied ESS

Implementation of PSO

The purposed algorithm PSO implemented to subsequent studies as

WES allied modified IEEE 57 bus system

The PSO has been implemented to inspection system, the real power loss has been dramatically reduced compared to the symmetry circumstance to the application of OPF. As of the Table 14 loss in real power is 11.848 MW, while the contribution from the wind is 226 MW in this state the functioning cost of the system is \$ 19007.4/ hour. The voltage profile of the buses is admirable around the value of 1.01 pu as disclosed in Table 11.

PSO					
WIND POWER	0 (MW)	14.54 (MW)	55.79 (MW)	98.12 (MW)	113 (MW)
BUS	Voltage (p.u)	Voltage (p.u)	Voltage (p.u)	Voltage (p.u)	Voltage (p.u)
1	1.0400	1.0400	1.0400	1.0400	1.0400
2	1.0100	1.0100	1.0100	1.0100	1.0100
3	0.9850	0.9850	0.9850	0.9850	0.9850
4	0.9867	0.9772	0.9777	0.9774	0.9775
5	0.9759	0.9728	0.9732	0.9729	0.9730
6	0.9800	0.9800	0.9800	0.9800	0.9800
7	0.9567	0.9808	0.9810	0.9809	0.9809
8	0.9587	1.0050	1.0050	1.0050	1.0050
9	0.9800	0.9800	0.9800	0.9800	0.9800
10	0.9822	0.9806	0.9809	0.9809	0.9809
11	0.9678	0.9655	0.9660	0.9660	0.9659
12	1.0150	1.0150	1.0150	1.0150	1.0150
13	0.9712	0.9678	0.9685	0.9684	0.9684
14	0.9611	0.9561	0.9569	0.9569	0.9568
15	0.9770	0.9736	0.9744	0.9744	0.9743
16	0.9964	0.9961	0.9968	0.9968	0.9967
17	0.9979	0.9975	0.9984	0.9983	0.9983
18	1.0762	0.9951	0.9957	0.9953	0.9955
19	1.2998	0.9632	0.9638	0.9636	0.9636
20	1.1776	0.9558	0.9564	0.9564	0.9563
21	1.0500	0.9940	0.9950	0.9948	0.9948
22	1.0206	0.9950	0.9960	0.9958	0.9958
23	1.0180	0.9932	0.9942	0.9940	0.9940
24	0.9905	0.9804	0.9817	0.9812	0.9813
25	0.9711	0.9584	0.9599	0.9593	0.9594
26	0.9542	0.9471	0.9480	0.9476	0.9477
27	0.9591	0.9692	0.9701	0.9696	0.9697
28	0.9680	0.9845	0.9852	0.9848	0.9849

29	0.9767	0.9973	0.9980	0.9975	0.9976
30	0.9528	0.9392	0.9407	0.9401	0.9403
31	0.9299	0.9145	0.9159	0.9155	0.9155
32	0.9506	0.9334	0.9346	0.9343	0.9343
33	0.9483	0.9311	0.9322	0.9320	0.9320
34	0.9576	0.9395	0.9407	0.9404	0.9404
35	0.9656	0.9475	0.9486	0.9484	0.9484
36	0.9761	0.9580	0.9591	0.9589	0.9589
37	0.9864	0.9681	0.9691	0.9690	0.9689
38	1.0185	0.9989	0.9999	0.9997	0.9997
39	0.9840	0.9658	0.9669	0.9667	0.9667
40	0.9723	0.9546	0.9557	0.9555	0.9555
41	0.9891	0.9828	0.9836	0.9836	0.9835
42	0.9640	0.9552	0.9559	0.9558	0.9558
43	1.0031	0.9996	1.0002	1.0002	1.0001
44	1.0195	1.0033	1.0042	1.0041	1.0041
45	1.0352	1.0263	1.0270	1.0269	1.0269
46	1.0567	1.0473	1.0480	1.0480	1.0479
47	1.0349	1.0213	1.0221	1.0220	1.0220
48	1.0297	1.0145	1.0154	1.0153	1.0153
49	1.0354	1.0238	1.0246	1.0246	1.0245
50	1.0203	1.0117	1.0124	1.0124	1.0123
51	1.0457	1.0427	1.0433	1.0433	1.0432
52	0.9541	0.9708	0.9713	0.9710	0.9711
53	0.9484	0.9630	0.9635	0.9632	0.9633
54	0.9850	0.9935	0.9936	0.9936	0.9936
55	1.0306	1.0331	1.0330	1.0333	1.0331
56	0.9705	0.9593	0.9600	0.9599	0.9599
57	0.9694	0.9566	0.9573	0.9571	0.9572

Table 11. Voltage outline for altered IEEE 57 bus system with WES

WES and ESS associated in altered IEEE 57 bus system

In this context, the PSO has been examined over the estimated test system with the assimilation of ESS. The PSO has demarcated the position of ESS as to the buses 6, 8, 9 and 12 correspondingly. The entire capacity of ESS connected is 43.2 MW as specified in Table 12. In the test system, robust voltage outline has been observed as per Table 14. The size of ESS attached amid the execution by OPF is slighter than performance by PSO, nonetheless the operation cost of test system in PSO is economical of \$ 19202.40/hour versus \$ 19631.86/hour in OPF for the zero infiltration of the WES power. In PSO if the entire power of WES injected to the system the expenses is \$ 19005.00/hour against \$ 19117.20/hour for OPF as observed in the Tables 13 and 14 respectively .

PSO					
WIND POWER	0 (MW)	14.54 (MW)	55.79 (MW)	98.12 (MW)	113 (MW)
BUS	Voltage (p.u)	Voltage (p.u)	Voltage (p.u)	Voltage (p.u)	Voltage (p.u)
1	1.0400	1.0400	1.0400	1.0400	1.0400
2	1.0100	1.0100	1.0100	1.0100	1.0100
3	0.9850	0.9850	0.9850	0.9850	0.9850
4	0.9777	0.9783	0.9781	0.9778	0.9778
5	0.9732	0.9738	0.9736	0.9734	0.9733
6	0.9800	0.9800	0.9800	0.9800	0.9800
7	0.9812	0.9813	0.9810	0.9811	0.9812
8	1.0050	1.0050	1.0050	1.0050	1.0050
9	0.9800	0.9800	0.9800	0.9800	0.9800
10	0.9811	0.9813	0.9810	0.9809	0.9812
11	0.9664	0.9667	0.9663	0.9662	0.9665
12	1.0150	1.0150	1.0150	1.0150	1.0150
13	0.9691	0.9695	0.9690	0.9688	0.9692
14	0.9578	0.9582	0.9577	0.9573	0.9579
15	0.9753	0.9755	0.9753	0.9747	0.9754
16	0.9983	0.9985	0.9982	0.9977	0.9983
17	1.0000	1.0003	1.0000	0.9993	1.0001
18	0.9957	0.9963	0.9962	0.9957	0.9958
19	0.9645	0.9651	0.9644	0.9644	0.9645
20	0.9575	0.9582	0.9571	0.9573	0.9576
21	0.9957	0.9962	0.9958	0.9952	0.9958
22	0.9969	0.9974	0.9968	0.9963	0.9969
23	0.9951	0.9956	0.9950	0.9945	0.9951
24	0.9825	0.9832	0.9825	0.9819	0.9826
25	0.9608	0.9617	0.9609	0.9602	0.9609
26	0.9487	0.9492	0.9487	0.9482	0.9488
27	0.9704	0.9710	0.9705	0.9701	0.9705
28	0.9855	0.9860	0.9856	0.9853	0.9856
29	0.9982	0.9986	0.9983	0.9980	0.9983
30	0.9416	0.9426	0.9417	0.9410	0.9418
31	0.9169	0.9177	0.9169	0.9162	0.9170
32	0.9355	0.9362	0.9355	0.9350	0.9357
33	0.9332	0.9338	0.9331	0.9326	0.9333
34	0.9417	0.9423	0.9416	0.9411	0.9418
35	0.9496	0.9502	0.9495	0.9490	0.9497
36	0.9600	0.9606	0.9599	0.9595	0.9601
37	0.9701	0.9706	0.9700	0.9695	0.9702
38	1.0007	1.0012	1.0006	1.0002	1.0008
39	0.9678	0.9684	0.9677	0.9673	0.9679
40	0.9567	0.9573	0.9566	0.9561	0.9568
41	0.9843	0.9848	0.9842	0.9839	0.9844
42	0.9566	0.9570	0.9565	0.9562	0.9566
43	1.0007	1.0011	1.0006	1.0004	1.0008
44	1.0051	1.0055	1.0050	1.0045	1.0051
45	1.0277	1.0279	1.0277	1.0272	1.0278

46	1.0490	1.0493	1.0488	1.0485	1.0490
47	1.0230	1.0233	1.0229	1.0225	1.0231
48	1.0163	1.0167	1.0162	1.0158	1.0163
49	1.0255	1.0260	1.0254	1.0251	1.0256
50	1.0133	1.0137	1.0131	1.0129	1.0133
51	1.0438	1.0442	1.0437	1.0436	1.0439
52	0.9715	0.9719	0.9716	0.9714	0.9716
53	0.9636	0.9639	0.9636	0.9635	0.9637
54	0.9938	0.9939	0.9937	0.9937	0.9938
55	1.0332	1.0331	1.0329	1.0331	1.0331
56	0.9606	0.9609	0.9606	0.9602	0.9606
57	0.9579	0.9582	0.9579	0.9575	0.9579
Allocation of ESS	Bus 7/24.2 MW, Bus 22/19.4 MW, and Bus 47/14.8 MW				
Total size of ESS	58.4 MW				

Table 12. Voltage outline for altered IEEE 57 bus system with WES allied ESS

Wind Power (MW)	OPF			
	Total Real power loss (MW)		Operation Cost (\$/hr)	
	Exclusion of ESS	Inclusion of ESS	Exclusion of ESS	Inclusion of ESS
0	28.602	16.886	18831.86	19631.86
29.08	27.638	17.801	18678.52	19480.52
111.58	25.441	16.652	18636.12	19348.12
196.24	23.996	16.027	18579.30	19155.30
226	23.679	15.923	18421.20	19117.20

Table 13. Total real power loss and operation cost for altered IEEE 57 bus system

Wind Power (MW)	PSO			
	Total Real power loss (MW)		Operation Cost (\$/hr)	
	Exclusion of ESS	Inclusion of ESS	Exclusion of ESS	Inclusion of ESS
0	12.512	11.231	19005.40	19202.40
29.08	12.300	11.010	19035.20	19053.60
111.58	11.726	11.178	18997.40	19007.40
196.24	11.880	11.590	19017.40	19057.60
226	11.848	11.181	19007.4	19005.00

Table 14. Total real power loss and operation cost for altered IEEE 57 bus system

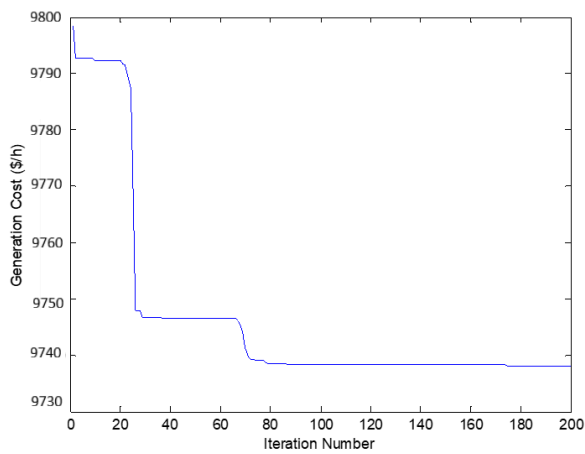


Fig 4: Correlation of expenses incurred by WES for 14.54 MW in the domain of OPF and PSO for IEEE 30 bus system

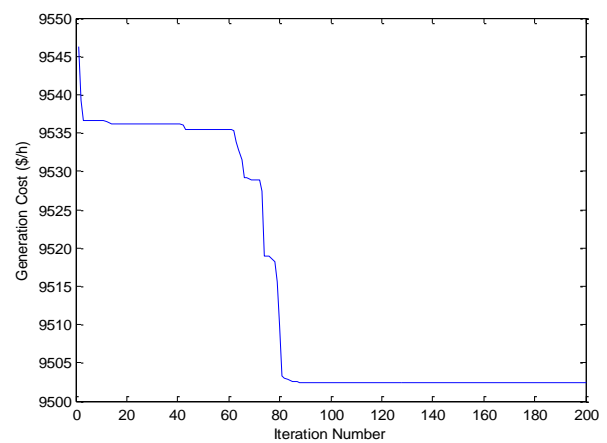
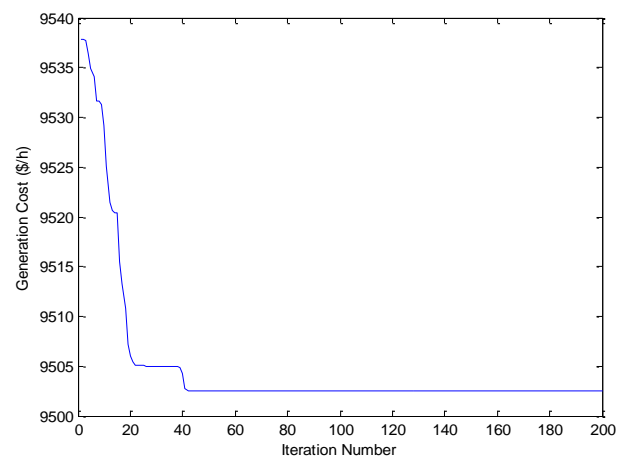
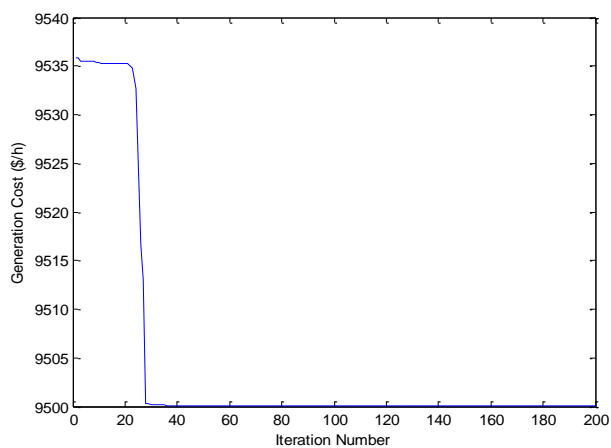


Fig 5: Correlation of expenses incurred by WES allied ESS for 14.54 MW in the domain of OPF and PSO for IEEE 30 bus system



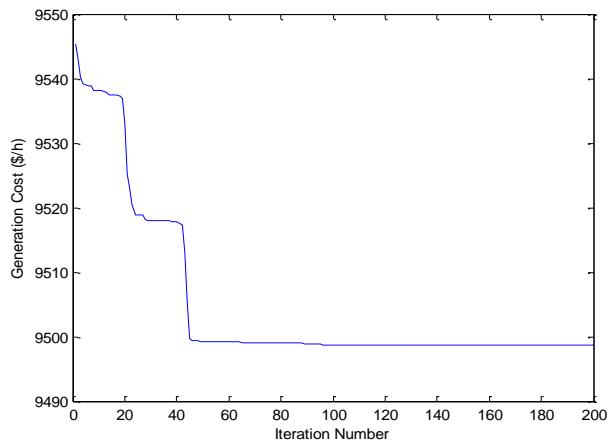


Fig 6: Correlation of expenses incurred by WECS allied ESS for 55.79 MW in the domain of OPF and PS

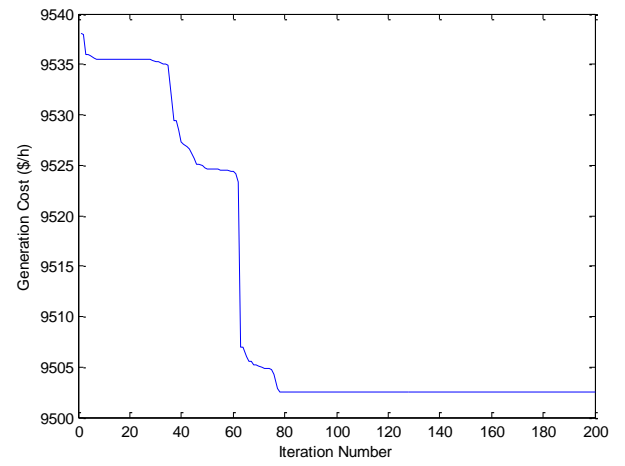


Fig 7: Correlation of expenses incurred by WECS allied ESS for 98.12 MW in the domain of OPF and PSO

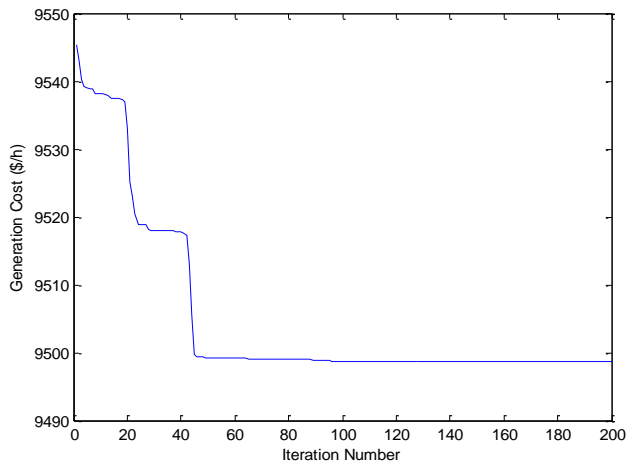
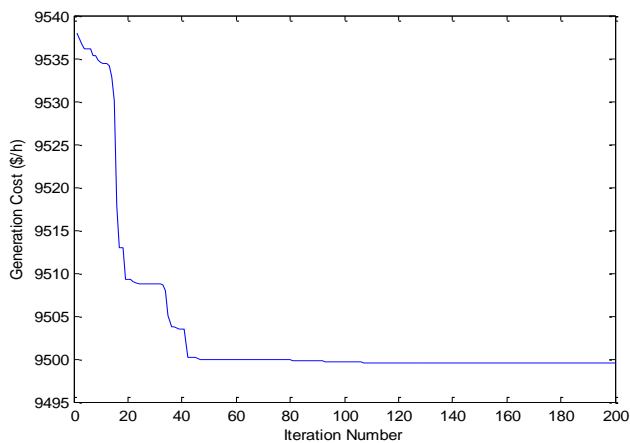
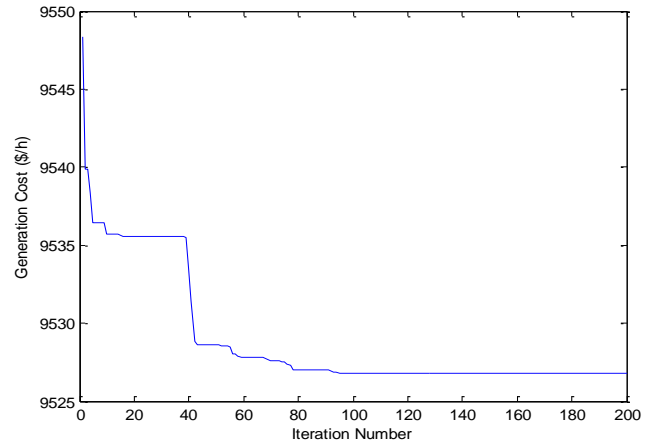


Fig 8: Correlation of expenses incurred by WECS allied ESS for 113 MW in the domain of OPF and PSO



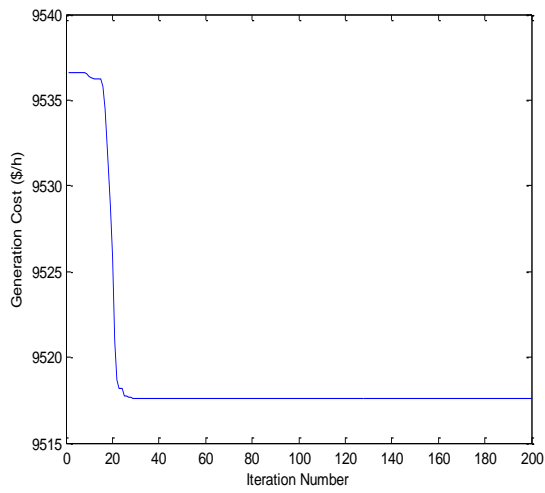


Fig 9: Correlation of expenses incurred by WES for 14.54 MW in the domain of OPF and PSO for IEEE 57 bus system.

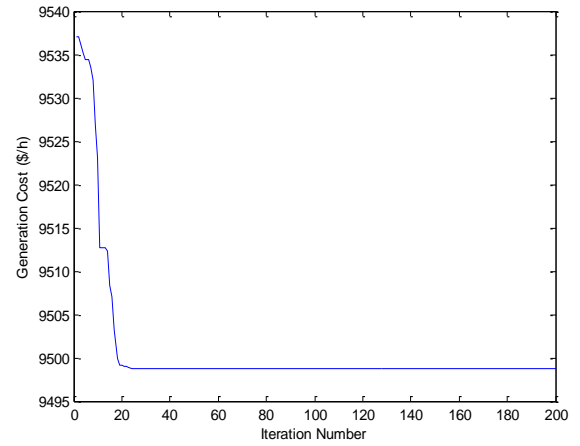
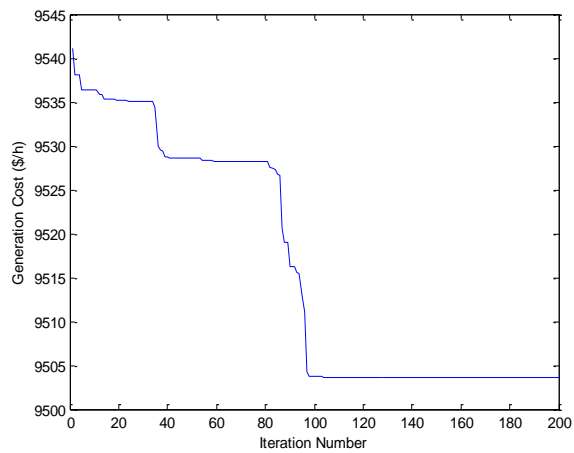


Fig 10: Correlation of expenses incurred by WES for 55.79 MW in the domain of OPF and PSO for IEEE 57 bus system.



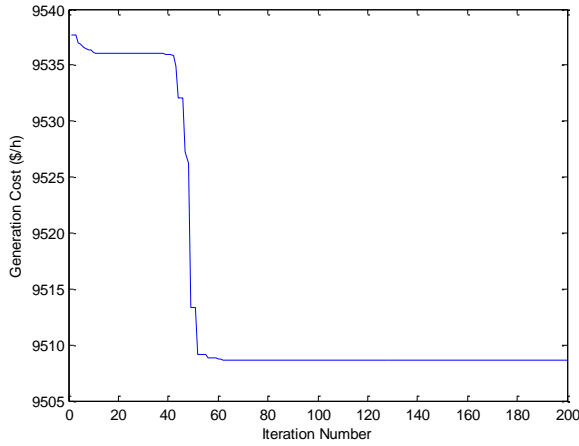


Fig 11: Correlation of expenses incurred by WES for 98.12 MW in the domain of OPF and PSO for IEEE 57 bus system.

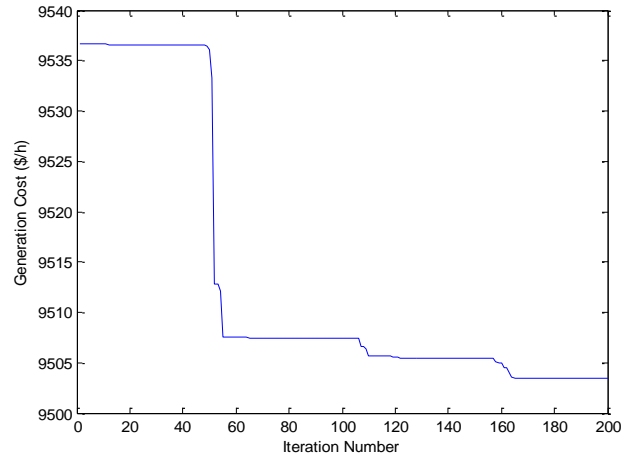
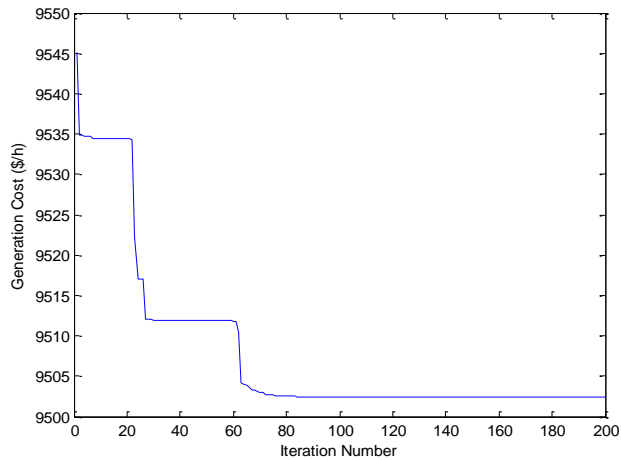


Fig 12: Correlation of expenses incurred by WES for 113 MW in the domain of OPF and PSO for IEEE 57 bus system.

CONCLUSION:

The effects of the coordination of wind power and Energy Storage Systems in three cases are examined and manifest with exhibit the adequacy of the proposed PSO strategy.

Case 1: A regular probabilistic load flow analysis for the system consider the entire wind power distribution, but without ESS installation.

Case 2: An optimal load flow (OPF) analysis to determine the best ESS allocation under the worst case scenario assuming zero wind power.

Case 3: A PSO analysis for the system consider the entire wind power distribution, but without ESS installation.

Case 4: PSO with ESS considering the entire wind distribution.

The parameters and conditions take after the information sheet in [20]. Six scenarios of wind power glean from Discrete Markov Analysis (DMA) are contemplated in these three contextual Analyses.

Case 1: The resultant bus voltages, operation cost, and losses of Case 1 are listed in Table 3. The highlighted rows represent the voltage of each generator.

It very well may be seen from Table 3 that the system operation cost and power misfortune lessens with the expansion of wind power. The total operation cost varies from 9815.93 \$/hr to 9458.6 \$/hr according to the changes of wind power from 0 to 113 MW.

Further, the system encounters both low-voltage and high voltage issues. At the point when the wind power is less than 55.79MW, the voltage at the wind generator bus practices a low-voltage issue. For particular, the voltage drops when the wind power is 0 MW. Under this circumstance, regardless of whether the voltages at the generator transports 11 and 13 are increased to 1.082 and 1.071 p.u. respectively, the low voltages still appear at buses 5, 8, 26 and 30.

Case 2: It can be seen from Table 4 that the system operation cost and power loss reduce with the increase of wind power. The Optimal Power Flow (OPF) analysis used to determine the real power loss and total cost. The total operation cost varies from 9832.1 \$/hr to 9509.5 \$/hr according to the changes of wind power from 0 to 113 MW. In this case, OPF is applied to analysis test system, the real power loss has been gradually declining when the wind power is admitted to the system progressively as in Table 7. Simultaneously, the operation cost of the appraisal system has been decreasing as summarized in Table 6. The voltage profile for this assumed test system is briefed in Table 4.

The UPQC implemented in Thirty-bus system has been successfully executed, modeled and simulated using MATLAB. The comparison of results of the thirty-bus system with and without UPQC is presented. The resemblance revealed that the real power losses are reduced by 6% by introducing the UPQC in the multi-bus system. The comparison of results of the thirty-bus system with & without UPQC indicates that the voltage stability is improved in the interconnected mode with UPQC.

The benefits of UPQC are sag mitigation, reduction of heat in the alternator & improvement of the voltage at load buses. The disadvantage of UPQC is that it requires a DC source to charge the DC link capacitor & the firing circuits have to be designed to operate at different frequencies.

REFERENCES:

1. Chen Peiyuan. Stochastic modeling and analysis of power system with renewable generator. Doctor of Philosophy. Aalborg University, Denmark; January 2010
2. Al-Bahadly Ibrahim. Wind turbines. InTech; 2011. p. 355–64 [chapter 15].
3. Keung Ping-Kwan, Kazachkov Yuriy, Senthil J. Generic models of wind turbines for power system stability studies. In: IEEE 8th international conference advances in power system control, operation and mainagement, Hong Kong; 2009. p.1–6.
4. Shamshad A, Bawadi MA, Wan Hussin WMA, Majid TA. First and second order markov chain models for synthetic generation of wind speed time series. *Energy* 2005;30:693–708.
5. Naik CA, Kundu P. Analysis of power quality disturbances using wavelet packet transform. In: IEEE 6th India international conference on power electronics (IICPE); 2014. p. 1–4.
6. Lee Soon, Park Jung-Wook, Venayagamoorthy Ganesh Kumar. New power quality index in a distribution power system by using RMP model. *IEEE Trans Ind Appl* 2010;46(3):1204–11.
7. Hajian Mahdi, Foroud Asghar Akbari, Abdoos Ali Akbar. New automated power quality recognition system for online/offline monitoring. *Neurocomputing* 2014;27:389–406.
8. Russo A, Varilone P, Caramia P. Point estimate schemes for probabilistic harmonic power flow. In: International conference on harmonics and quality of power (ICHQP); 2014. p. 19–23.
9. Li Lingling, Wang Minghui, Zhu Fenfen, Wang Chengshan. Wind power forecasting based on time series and neural network. *Int Comput Sci Comput Technol* 2009;293–7.
10. Gomes Pedro, Castro Rui. Wind speed and wind power forecasting using statistical models: AutoRegressive Moving Average (ARMA) and Artificial Neural Networks (ANN). *Int J Sustain Energy Dev* 2012;1:36–45.
11. Q. Fu, L. F. Montoya, A. Solanki, A. Nasiri, V. Bhavaraju, T. Abdallah, and D. C. Yu, “Microgrid generation capacity design with renewable and energy storage addressing power quality and surety,” *IEEE Trans. Smart Grid*, vol. 3, no. 4, pp. 2019–2027, 2012.
12. C. Lo and M. Anderson, “Economic dispatch and optimal sizing of battery energy storage systems in utility load-leveling operations,” *IEEE Trans. Energy Convers.*, vol. 14, no. 3, pp. 824–829, Sep. 1999.
13. C. Abbey and G. Joós, “A stochastic optimization approach to rating of energy storage systems in wind-diesel isolated grids,” *IEEE Trans. Power Syst.*, vol. 24, no. 2, pp. 418–426, Feb. 2009.

14. M. Nick, M. Hohmann, R. Cherkaoui, and M. Paolone, "On the optimal placement of distributed storage systems for voltage control in active distribution networks," in *Proc. 3rd IEEE PES Int. Conf. Exhibition Innovative Smart Grid Technol.*, 2012, pp. 1–6.
15. J. K. Kaldellis and D. Zafirakis, "Optimum energy storage techniques for the improvement of renewable energy sources-based electricity generation economic efficiency," *Energy*, vol. 32, no. 12, pp. 2295–2305, Dec. 2006.
16. Y. Xu and C. Singh, "Multi-objective design of energy storage in distribution systems based on modified particle swarm optimization," in *Proc. IEEE Power and Energy Soc. Gen. Meeting*, 2012, pp. 1–8.
17. N. Bazmohammadi, A. Karimpour, and S. Bazmohammadi, "Optimal operation management of a microgrid based on MOPSO and differential evolution algorithms," in *Proc. IEEE Smart Grids Meeting*, 2012, pp. 1–6.
18. P. Jong-Bae, J. Yun-Won, S. Joong-Rin, and K. Y. Lee, "An improved particle swarm optimization for nonconvex economic dispatch problems," *IEEE Trans. Power Syst.*, vol. 25, no. 1, pp. 156–166, Feb. 2010.
19. C. Zhang, M. Chen, and C. Luo, "A multi-objective optimization method for power system reactive power dispatch," in *Proc. IEEE Intell. Control Automation*, 2010, pp. 6–10.
20. K. Deb, *Multi-Objective Optimization Using Evolutionary Algorithms*. Singapore: Wiley, 2003.
21. "30 Bus Power Flow Test Case," Univ. Washington [Online]. Available: http://www.ee.washington.edu/research/pstca/pf30/pg_tca30bus.htm.
22. S. Sooriyaprabha and Dr. C. K. Babulal, "Synthetic wind speed model and probabilistic power quality indices for electric grid with wind power generation," *IEEE Trans. Power Syst.*
23. J. Kennedy and R. Eberhart, "Particle swarm optimization," in *Proc. IEEE Int. Conf. Neural Networks*, Piscataway, NJ, USA, 1995, pp. 1942–1948.
24. R. Eberhart and J. Kennedy, "A new optimizer using particle swarm theory," in *Proc. 6th Int. Symp. Micro Machine and Human Sci.*, 1995, pp. 39–43.
25. X. Hu, Y. Shi, and R. Eberhart, "Recent advances in particle swarm," in *Proc. Congr. Evol. Computation*, 2004, vol. 1, pp. 90–97.
26. Shuli Wen et al., "Economic allocation for energy storage system considering wind power distribution," *IEEE Trans. Power Syst.*
27. Khaled M. Abo-Al-Ez, Mohammed G. Osman, Sahar S. Kaddah, and Tamer F. Megahed, (2016) "Probabilistic power quality indices for electric grids with increased penetration level of wind power generation," *ELSEVIER Electrical Power and Energy Systems*, Vol. 77, no. 50–58.
28. Kamble, S. Y., Waware, M. M. (2013) "Unified power quality conditioner for power quality improvement with advanced control strategy" *IEEE International Multi Conference on Automation, Computing, Control, Communication and Compressed Sensing* on (March) 22–23, pp. 432 – 437, 22–23.
29. Chandra. A and Khadkikar. V (2011) "UPQC-S: A novel concept of simultaneous voltage sag/swell and load reactive power compensations utilizing series inverter of UPQC," *IEEE Trans. Power Electron.*, (Sep) vol. 26, no. 9, pp. 2414–242.
30. Kameswara Rao. R and Tulasiram S. S., "Harmonic modeling of residential and commercial loads with unified power quality conditioner," *International journal of scientific & engineering research*, vol. 3, issue 6, June) 1, ISSN 2229-5518.
31. Dixon J, Moran L, Pastonini I and Wallace R, (2006) "Series active power filter compensates current harmonics and voltage unbalance simultaneously," *Proc. IEE Gener., Trans. and Distrib.*, (Jan) Vol. 147, No. 1, pp. 31–36.
32. Chen Jian Chen, Duan Shanxu and Li. Xun, Zhu. Guorong, (2007) "Control scheme for three-phase four wire UPQC in a three-phase stationary frame," *Proc. IEEE/IECON 2007*, pp. 1732–1736.
33. Khadkikar V, (2012) "Enhancing Electric Power Quality Using UPQC: A comprehensive overview," *IEEE Trans, Power Electron.* (May) Vol. 27, No. 5. Pp. 2284 – 2297..
34. Chen Jian, Duan Shanxu Tan Zhili, Kang Yong and, Li Xun, "A direct control strategy for UPQC in three-phase four-wire system," *Proc.*

- IEEE Conf. on Power Electronics and Motion Control 2006, vol. 2, pp. 1-5.
35. . Teke, L. Saribulut and Tumay M,(2011) “A novel reference signal generation method for power quality improvement of unified power quality conditioner,” IEEE Trans. Power Del.(Oct), Vol. 26, no. 4, pp. 2205-2214.
 36. Akagi H. and Fujita H,(1998) “The unified power quality conditioner: The integration of series and shunt active filters,” IEEE Trans. Power Electron.,(Mar) vol. 13, no. 2, pp. 315-322.
 37. Akagi H, Aredes M and Watanabe E H(2007) “Instantaneous power theory and applications to power conditioning,(Apr.)” Hoboken, NJ: Wiley IEEE Press.
 38. Akagi. H(1996), “New trends in active filters for power conditioning,” IEEE Trans. Ind. Applicat.,(Nov/Dec) vol. 32, pp. 1312-1332,.
 39. Ghosh A and Ledwich G,(2001) “A unified power quality conditioner (UPQC) for simultaneous voltage and current compensation,” Elect. Power Syst. Res., pp. 55-63.
 40. Chen Peiyuan (2010), Stochastic modeling and analysis of power system with renewable generator. Doctor of Philosophy. Aalborg University, Denmark;
 41. Abo-al-ez Khaled M, Elaiw Ahmed, Xia Xiaohua. A dual-loop model predictive voltage control/sliding-mode current control for voltage source inverter operation in smart microgrids. Electr Power Compon Syst 2014;423-:348–60.
 42. Kundu P and Naik C A. Analysis of power quality disturbances using wavelet packettransform. In: IEEE 6th India international conference on power electronics(IICPE);
 43. Ganesh Kumar ,Lee Soon, Park Jung-Wook andVenayagamoorthy. New power quality index in a distribution power system by using RMP model. IEEE Trans Ind Appl 2010;46(3):1204–11
 44. Hajian Mahdi, Foroud Asghar Akbari, Abdoos Ali Akbar. New automated powerquality recognition system for online/offline monitoring. Neurocomputing 2014;27:389–406.
 45. Caramia P ,Russo A and Varilone P,. Point estimate schemes for probabilistic harmonic power flow. In: International conference on harmonics and quality of power (ICHQP); 2014. p. 19–23.
 46. Li Lingling, Wang Chengshan Wang Minghui and Zhu Fenfen,. Wind power forecasting based on time series and neural network. Int Comput Sci Comput Technol 2009:293–7.
 47. Castro Rui and Gomes Pedro,. Wind speed and wind power forecasting using statistical models: AutoRegressive Moving Average (ARMA) and Artificial Neural Networks (ANN). Int J Sustain Energy Dev 2012;1:36–45.
 48. Bawadi MA, Majid TA Shamshad A and Wan Hussin WMA,. First and second order markov chain models for synthetic generation of wind speed time series.Energy 2005;30:693–708.